



**HAL**  
open science

# Hybrid geometric calibration in 3D cone-beam with sources on a plane

Anastasia Konik, Laurent Desbat, Yannick Grondin

► **To cite this version:**

Anastasia Konik, Laurent Desbat, Yannick Grondin. Hybrid geometric calibration in 3D cone-beam with sources on a plane. 17th International Meeting on Fully 3D Image Reconstruction in Radiology and Nuclear Medicine, Stony Brook University, Jul 2023, Stony Brook, United States. pp.207-210. hal-04265482

**HAL Id: hal-04265482**

**<https://hal.science/hal-04265482>**

Submitted on 30 Oct 2023

**HAL** is a multi-disciplinary open access archive for the deposit and dissemination of scientific research documents, whether they are published or not. The documents may come from teaching and research institutions in France or abroad, or from public or private research centers.

L'archive ouverte pluridisciplinaire **HAL**, est destinée au dépôt et à la diffusion de documents scientifiques de niveau recherche, publiés ou non, émanant des établissements d'enseignement et de recherche français ou étrangers, des laboratoires publics ou privés.

# Hybrid Geometric Calibration in 3D Cone-Beam with Sources on a Plane

Anastasia Konik<sup>1</sup>, Laurent Desbat<sup>1</sup>, and Yannick Grondin<sup>2</sup>

<sup>1</sup>TIMC-GMCAO, Université Grenoble Alpes, Grenoble, France

<sup>2</sup>SurgiQual Institute, Meylan, France

**Abstract** In this work, we describe a new self-calibration algorithm in the case of 3D cone-beam geometry with sources on a plane parallel to the detector plane. This algorithm is hybrid, so it combines data consistency conditions (DCCs) and the partial knowledge on the pattern of the calibration cage. We explain how we build this algorithm with the modelling of calibration markers by Diracs and the generalization of existing DCCs for this geometry to distributions. This new method can work with truncated projections if the marker projections are not truncated. With this hybrid approach, we build an analytical self-calibration algorithm based on DCCs, robust to projection truncations. We show numerical experiments.

## 1 Introduction

In the recent work [1] a hybrid approach to calibrate a cone-beam system was proposed. This method combines data consistency conditions (DCCs), special equations on projection data, and detected anatomical markers. We continued the development of similar methods and presented hybrid methods in 2D fan-beam geometry and 3D cone-beam geometry, both with sources on a line, see [2, 3]. In our approaches we modelled the calibration markers by Dirac distributions and exploited DCCs on distributions. Compared with [1], our calibration algorithms with such DCCs are analytical, thus we don't need to solve numerical optimization procedures. Moreover, because we use DCCs only on markers, the projection data may be truncated. Only the marker projections must be non-truncated. Thus, moment conditions of DCCs on the set of Diracs yields the extension of existing calibration procedures based on DCCs to truncated projections.

In [4] DCCs for functions were proposed for the 3D cone-beam with sources on a plane parallel to the detector plane. In this work, we show that the generalisation of these DCCs to distributions helps to overcome difficulties in the construction of the analytical calibration procedure for this geometry and allows the hybrid geometric self-calibration with truncated data.

## 2 Calibration problem

3D divergent X-ray systems lead to the cone-beam projection data defined by the following transform:

**Definition 2.1.** *The cone-beam transform of the function  $f$  of compact support describing an object is*

$$\mathfrak{D}f(\vec{s}_\lambda, \vec{\zeta}) := \int_0^{+\infty} f(\vec{s}_\lambda + l\vec{\zeta})dl, \quad (1)$$

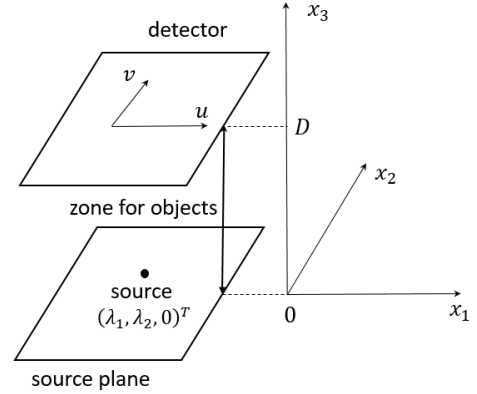


**Figure 1:** The cone-beam geometry with sources on a plane parallel to the detector.

where  $\lambda \in \mathbb{R}$  is the trajectory parameter of the source  $\vec{s}_\lambda \in \mathbb{R}^3$  and the (usually unit) vector  $\vec{\zeta}$  is the direction of the integration line.

For the cone-beam transform with sources on a plane parallel to the detector, we work with the geometry presented in the Figure 1, see also [4]. Here we have sources moving in a plane parallel to the detector plane: the source trajectory is  $\vec{s}_\lambda = (\lambda_1, \lambda_2, 0)^T$ , the detector is in  $x_3 = D$ , the non-unit direction of the integration line  $\vec{\zeta} = (u, v, D)^T - (\lambda_1, \lambda_2, 0)^T$ ,  $u$  and  $v$  are parameters of the detector. In this case we can rewrite our data as:

**Definition 2.2.** *The cone-beam transform with sources on a plane parallel to the detector plane of a function  $f$  of compact support between the source plane  $x_3 = 0$  and the detector plane  $x_3 = D$  is*

$$\mathfrak{D}f(\lambda_1, \lambda_2, u, v) := \int_0^{+\infty} f(\lambda_1 + l(u - \lambda_1), \lambda_2 + l(v - \lambda_2), lD)dl. \quad (2)$$

We can denote the cone-beam transform for fixed  $\lambda_1$  and  $\lambda_2$  with  $\mathfrak{D}_{\lambda_1, \lambda_2}f(u, v) := \mathfrak{D}f(\lambda_1, \lambda_2, u, v)$  for  $f$  with support in  $Y_3 = \mathbb{R}^2 \times (D_1, D_2)$ ,  $0 < D_1 < D_2 < D$ . Then we consider  $\mathfrak{D}_{\lambda_1, \lambda_2}f$  as a function of two variables.

Suppose that we work with a lattice of  $u, v$ , but the system is moving. So, we don't know exactly:

- source positions  $\lambda_{1i}$  and  $\lambda_{2i}$  for  $P$  projections,  $i \in \llbracket 0, P-1 \rrbracket$ ,
- detector shifts  $u_i, v_i$  for each source position  $i$ .

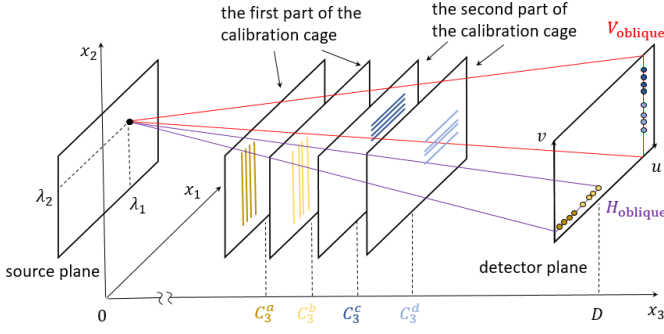


**Figure 2:** The 3D cone-beam geometry with sources on a plane with the calibration cage of two groups of 8 parallel sticks each.

We know  $m_i(u, v)$ , where  $m_i(u, v) = \mathcal{D}_{\lambda_{1i}, \lambda_{2i}} f(u - u_i, v - v_i)$ . We need to estimate the geometric calibration parameters  $\lambda_{1i}$ ,  $\lambda_{2i}$ ,  $u_i$ ,  $v_i$ ,  $i \in \llbracket 0, P-1 \rrbracket$ . We want to do it with the specific calibration cage presented in the Figure 2. So, we add some calibration object with unknown position. We want to use DCCs on projections of this object to perform the full analytical calibration.

Our task can be separated into two independent tasks to find the couple of  $\lambda_{1i}$  and  $u_i$  for the first task with the help of the first part of the calibration cage (8 vertical sticks) and  $\lambda_{2i}$  and  $v_i$  for the second task with the second part of the calibration cage (8 horizontal sticks).

We place these sticks as close as possible to the detector and two groups of sticks are separated such that it's possible to select one horizontal detector line for the vertical sticks and one vertical detector line for horizontal sticks containing only projections of one part of our calibration cage. Thus, it's possible to work separately with the projection of vertical sticks for one fixed detector line and the projection of horizontal sticks for another fixed detector column. So, we can say that we need to select two appropriate detector lines (one horizontal and one vertical) for the current source position or two oblique planes (one horizontal  $H_{\text{oblique}}$  and one vertical  $V_{\text{oblique}}$ ) passing through each detector line and the current source position. Let us consider the intersection of sticks with one selected oblique plane and points of the calibration cage in this intersection as Dirac distributions.

For each group of 8 sticks we have a known pattern, the same as we used in our previous works [2, 3]. Let us consider only the first vertical group of sticks (the same can be written for the second group). Each subgroup of 4 sticks belongs to one plane. Let us use the superscript  $l = a$  or  $l = b$  for each group of 4 sticks. We have more unknowns in our calibration problem:

- the first 4 sticks are in the unknown plane  $x_3 = C_3^a$ , the second 4 sticks are in the unknown plane  $x_3 = C_3^b$ ,
- we suppose that sticks are perpendicular to the  $x_1$ -axis, then points in the intersection of sticks and the fixed oblique plane  $H_{\text{oblique}}$  are  $c_{11}^a = p_a - k_1 L$ ,  $c_{21}^a = p_a - L$ ,  $c_{31}^a = p_a + L$ ,  $c_{41}^a = p_a + k_1 L$ ,  $c_{11}^b = p_b - k_2 L$ ,  $c_{21}^b =$

$p_b - k_3 L$ ,  $c_{31}^b = p_b + k_3 L$ ,  $c_{41}^b = p_b + k_2 L$ , where  $p_a$ ,  $p_b$  are unknown and define the  $x_1$ -position of the center of mass of each subgroup,  $L$ ,  $k_1 > 0$ ,  $k_2 > 0$ ,  $k_3 > 0$  are known; we also assume that  $D$  is known.

Thus, by knowing the abscissas  $q_{ij}^l$  ( $i \in \llbracket 0, P-1 \rrbracket$ ,  $j \in \llbracket 1, 4 \rrbracket$ ,  $l \in \{a, b\}$ ), the detected projections of the stick intersections with the oblique plane  $H_{\text{oblique}}$ , for one fixed detector line and some parameters of the pattern of the calibration cage (see previous paragraph), we want to identify the geometrical calibration parameters  $\lambda_{1i}$ ,  $u_i$ ,  $i \in \llbracket 0, P-1 \rrbracket$ , and the unknown position of the calibration cage  $p_a$ ,  $p_b$ ,  $C_3^a$ ,  $C_3^b$ . With essentially the same procedure (see the next section), but the vertical oblique plane and 8 horizontal sticks, we identify  $\lambda_{2i}$ ,  $v_i$ ,  $i \in \llbracket 0, P-1 \rrbracket$ ,  $p_c$ ,  $p_d$ ,  $C_3^c$ ,  $C_3^d$ .

### 3 Hybrid solution

The mathematical theory of the cone-beam transform on distributions with sources on a plane parallel to the detector allowed to build the similar hybrid algorithm that we used in our previous works [2, 3], see section 4.

Let us define  $r_a = \frac{D - C_3^a}{C_3^a}$ ,  $r_b = \frac{D - C_3^b}{C_3^b}$ . It was possible to derive analytical formulas to calibrate with DCCs in this case (for the first task, the similar algorithm can be constructed for the second task):

1.  $r_a$  and  $r_b$  can be uniquely estimated from

$$\begin{cases} \sum_{j=1}^4 (q_{ij}^a)^2 = (1 + r_a)^2 (2 + 2k_1^2) L^2 + K_a(i) \\ \sum_{j=1}^4 (q_{ij}^b)^2 = (1 + r_b)^2 (2k_2^2 + 2k_3^2) L^2 + K_b(i), \end{cases} \quad (3)$$

where

$$K_l(i) = \frac{1}{4} \left[ \sum_{j=1}^4 q_{0j}^l \right]^2 + 2\Delta\tilde{M}_1^l(i) \sum_{j=1}^4 q_{0j}^l + 4[\Delta\tilde{M}_1^l(i)]^2,$$

$$\Delta\tilde{M}_1^l(i) = \frac{1}{4} \left( \sum_{j=1}^4 q_{ij}^l - \sum_{j=1}^4 q_{0j}^l \right),$$

and then we can deduce  $C_3^a$  and  $C_3^b$  from  $r_a$  and  $r_b$ ,

2.  $p_a$  and  $p_b$  can be estimated from

$$\sum_{j=1}^4 q_{0j}^l = (1 + r_l) 4p_l, \quad l \in \{a, b\}, \quad (4)$$

3. from the linear system

$$u_i - \lambda_{1i} r_l = \Delta\tilde{M}_1^l(i) \quad (5)$$

we compute  $u_i$  and  $\lambda_{1i}$  for each projection: (5) gives us 2 equations with 2 unknowns, since  $l \in \{a, b\}$ .

#### 4 Mathematical basis

In this section we describe the theory that we built and used in the derivation of our algorithm. Firstly, we generalize the definition of the cone-beam transform from the second section to distributions. Then we provide the generalization of known DCCs given in [4] to distributions.

**Definition.** Denote for any open set  $\Omega_N \subset \mathbb{R}^N$  the spaces of compactly supported smooth functions  $\mathcal{D}(\Omega_N)$ , the spaces of smooth functions  $\mathcal{E}(\Omega_N)$ ,  $N \in \{2, 3\}$ . Then  $\mathcal{D}'(\Omega_N)$  and  $\mathcal{E}'(\Omega_N)$  state for the sets of corresponding distributions.

We need to define the dual operator  $\mathfrak{D}_{\lambda_1, \lambda_2}^*$  of  $\mathfrak{D}_{\lambda_1, \lambda_2}$ . For  $f \in \mathcal{D}(\mathbb{R}^3)$  and  $\phi \in \mathcal{E}(\mathbb{R}^2)$ :

$$\begin{aligned} (\mathfrak{D}_{\lambda_1, \lambda_2} f, \phi) &= \int_{\mathbb{R}^2} \mathfrak{D}_{\lambda_1, \lambda_2} f(u, v) \phi(u, v) dudv \\ &= \int_{\mathbb{R}^2} \int_0^{+\infty} f(\lambda_1 + l(u - \lambda_1), \lambda_2 + l(v - \lambda_2), lD) dl \phi(u, v) dudv \\ &= \frac{1}{D} \int_{\mathbb{R}^2} \int_0^{+\infty} f\left(\lambda_1 + \frac{t_3}{D}(u - \lambda_1), \lambda_2 + \frac{t_3}{D}(v - \lambda_2), t_3\right) dt_3 \\ &\quad \times \phi(u, v) dudv = \int_0^{+\infty} \int_{\mathbb{R}^2} f(t_1, t_2, t_3) \\ &\quad \times \phi\left(\frac{Dt_1 - \lambda_1(D - t_3)}{t_3}, \frac{Dt_2 - \lambda_2(D - t_3)}{t_3}\right) \frac{D}{t_3^2} dt_1 dt_2 dt_3 \\ &= \langle f, \mathfrak{D}_{\lambda_1, \lambda_2}^* \phi \rangle, \quad (6) \end{aligned}$$

where  $(\cdot, \cdot)$  is the scalar product in  $L^2(\mathbb{R}^2)$ ,  $\langle \cdot, \cdot \rangle$  is the scalar product in  $L^2(Y_3)$ , we used the change of variables  $t_3 = lD$ ,  $dl = \frac{dt_3}{D}$ ;  $t_1 = \lambda_1 + \frac{t_3}{D}(u - \lambda_1)$ ,  $du = \frac{D}{t_3} dt_1$ ;  $t_2 = \lambda_2 + \frac{t_3}{D}(v - \lambda_2)$ ,  $dv = \frac{D}{t_3} dt_2$ .

We can define the dual operator for functions from  $\mathcal{E}(\mathbb{R}^2)$ :

$$\mathfrak{D}_{\lambda_1, \lambda_2}^* \phi(\vec{x}) := \frac{D}{x_3^2} \phi\left(\frac{Dx_1 - \lambda_1(D - x_3)}{x_3}, \frac{Dx_2 - \lambda_2(D - x_3)}{x_3}\right). \quad (7)$$

**Definition 4.1.** The cone-beam transform on a plane at fixed  $\lambda_1$  and  $\lambda_2$  of a compactly supported distribution  $f \in \mathcal{E}'(Y_3)$  is a distribution from  $\mathcal{E}'(\mathbb{R}^2)$  defined by the dual equality

$$(\mathfrak{D}_{\lambda_1, \lambda_2} f, \phi) = \langle f, \mathfrak{D}_{\lambda_1, \lambda_2}^* \phi \rangle \quad (8)$$

with the dual operator from (7).

Since we model the intersection at  $\vec{c}$  of a projection line with an opaque stick by a Dirac distribution  $\delta_{\vec{c}}$ , then

$$\begin{aligned} (\mathfrak{D}_{\lambda_1, \lambda_2} \delta_{\vec{c}}(u, v), \phi(u, v)) &= \langle \delta_{\vec{c}}(\vec{x}), \mathfrak{D}_{\lambda_1, \lambda_2}^* \phi(\vec{x}) \rangle \\ &= \left\langle \delta_{\vec{c}}(\vec{x}), \frac{D}{x_3^2} \phi\left(\frac{Dx_1 - \lambda_1(D - x_3)}{x_3}, \frac{Dx_2 - \lambda_2(D - x_3)}{x_3}\right) \right\rangle \\ &= \frac{D}{c_3^2} \phi\left(\frac{Dc_1 - \lambda_1(D - c_3)}{c_3}, \frac{Dc_2 - \lambda_2(D - c_3)}{c_3}\right) = \frac{D}{c_3^2} \delta_{\vec{c}}(\phi), \\ \text{where } \vec{c} &= \left(\frac{Dc_1 - \lambda_1(D - c_3)}{c_3}, \frac{Dc_2 - \lambda_2(D - c_3)}{c_3}\right). \quad (9) \end{aligned}$$

It's easy to see that  $\tilde{c}$  is the perspective projection of  $\vec{c}$  in the geometry of  $\mathfrak{D}_{\lambda_1, \lambda_2}$ .

For the sum of Diracs  $f = \sum_{j=1}^n \delta_{\tilde{c}_j}$

$$\begin{aligned} \mathfrak{D}_{\lambda_1, \lambda_2} f &= \sum_{j=1}^n \frac{D}{c_{j3}^2} \delta_{\tilde{c}_j}, \\ \tilde{c}_j &= \left(\frac{Dc_{j1} - \lambda_1(D - c_{j3})}{c_{j3}}, \frac{Dc_{j2} - \lambda_2(D - c_{j3})}{c_{j3}}\right). \quad (10) \end{aligned}$$

**DCCs.** The DCCs for functions from [4] state:

**Theorem 4.1.** Define

$$J_k(\lambda_1, \lambda_2, U, V) = \int_{-\infty}^{+\infty} g(\lambda_1, \lambda_2, u, v) (uU + vV)^k dudv \quad (11)$$

for all  $k = 0, 1, 2, \dots$ . Then  $J_k(\lambda_1, \lambda_2, U, V) = \mathcal{P}_k(U, V, -\lambda_1 U - \lambda_2 V)$ ,  $\mathcal{P}_k(U, V, W)$  is a homogeneous polynomial of degree  $k$  and  $g(\lambda_1, \lambda_2, \cdot, \cdot)$  has a compact support for all  $(\lambda_1, \lambda_2)$  if and only if  $g = \mathfrak{D}f$  with compactly supported  $f$  in  $z > 0$ .

We can generalize the necessary part of these DCCs to distributions of compact support:

**Theorem 4.2.** If  $f \in \mathcal{E}'(Y_3)$ ,  $g_{\lambda_1, \lambda_2} = \mathfrak{D}_{\lambda_1, \lambda_2} f$  is the cone-beam transform on a plane of  $f$  for fixed  $\lambda_1, \lambda_2$ , then:

1.  $g_{\lambda_1, \lambda_2} \in \mathcal{E}'(\mathbb{R}^2)$ ,
2. for  $k = 0, 1, 2, \dots$  we have the moment conditions:

$$(g_{\lambda_1, \lambda_2}(u, v), (uU + vV)^k) = \mathcal{P}_k(U, V, -\lambda_1 U - \lambda_2 V), \quad (12)$$

where  $\mathcal{P}_k(U, V, W)$  is a homogeneous polynomial of degree  $k$ .

*Proof.* Let us prove here the moment conditions that we plan to use. Obviously  $(u, v) \mapsto (uU + vV)^k \in \mathcal{E}(\mathbb{R}^2)$ , then

$$\begin{aligned} (\mathfrak{D}_{\lambda_1, \lambda_2} f(u, v), (uU + vV)^k) &= \langle f(\vec{x}), \mathfrak{D}_{\lambda_1, \lambda_2}^* ((uU + vV)^k)(\vec{x}) \rangle \\ &= \left\langle f(\vec{x}), \frac{D}{x_3^2} \left(\frac{Dx_1 - \lambda_1(D - x_3)}{x_3} U + \frac{Dx_2 - \lambda_2(D - x_3)}{x_3} V\right)^k \right\rangle \\ &= \left\langle f(\vec{x}), \frac{D}{x_3^{k+2}} (Dx_1 U + Dx_2 V + (D - x_3)(-\lambda_1 U - \lambda_2 V))^k \right\rangle \\ &= \left\langle f(\vec{x}), \frac{D}{x_3^{k+2}} \sum_{\substack{i, j, l \\ i+j+l=k}} \frac{k!}{i!j!l!} (Dx_1 U)^i (Dx_2 V)^j \right. \\ &\quad \left. \times ((D - x_3)(-\lambda_1 U - \lambda_2 V))^l \right\rangle = \sum_{\substack{i, j, l \\ i+j+l=k}} \frac{k!}{i!j!l!} U^i V^j \\ &\quad \times (-\lambda_1 U - \lambda_2 V)^l \left\langle f(\vec{x}), \frac{D}{x_3^{k+2}} (Dx_1)^i (Dx_2)^j (D - x_3)^l \right\rangle \\ &= \mathcal{P}_k(U, V, -\lambda_1 U - \lambda_2 V). \quad \square \end{aligned}$$

**Non-uniqueness of the solution.** Let  $f_{M,\vec{r}}(\vec{x}) := f(M\vec{x} + \vec{r})$

with  $M = \begin{pmatrix} 1 & 0 & -(u' + \lambda'_1)/D \\ 0 & 1 & -(v' + \lambda'_2)/D \\ 0 & 0 & 1 \end{pmatrix}$  and  $\vec{r} = (\lambda'_1, \lambda'_2, 0)^T$ , then

it can be shown for functions

$$\mathfrak{D}f_{M,\vec{r}}(\lambda_1, \lambda_2, u, v) = \mathfrak{D}f(\lambda_1 + \lambda'_1, \lambda_2 + \lambda'_2, u - u', v - v'). \quad (13)$$

It can be generalized to distributions  $f = \delta_{\vec{c}} \in \mathcal{E}'(Y_3)$ . Let us

define  $f_{M,\vec{r}} \in \mathcal{E}'(Y_3)$  as  $\langle f_{M,\vec{r}}(\vec{x}), \phi(\vec{x}) \rangle = \langle f(\vec{x}), \phi(M^{-1}(\vec{x} - \vec{r})) \rangle$ , where  $M^{-1} = \begin{pmatrix} 1 & 0 & (u' + \lambda'_1)/D \\ 0 & 1 & (v' + \lambda'_2)/D \\ 0 & 0 & 1 \end{pmatrix}$ , thus  $M^{-1}(\vec{x} - \vec{r}) = \begin{pmatrix} x_1 - \lambda'_1 + \frac{u' + \lambda'_1}{D}x_3 \\ x_2 - \lambda'_2 + \frac{v' + \lambda'_2}{D}x_3 \\ x_3 \end{pmatrix}$ . Then  $(\delta_{\vec{c}})_{M,\vec{r}}$  is the distribution

$\delta_{M^{-1}(\vec{c} - \vec{r})} \in \mathcal{E}'(Y_3)$ . Then it's easy to show

$$\begin{aligned} & (\mathfrak{D}_{\lambda_1, \lambda_2} (\delta_{\vec{c}})_{M,\vec{r}}(u, v), \phi(u, v)) = \\ & = (\mathfrak{D}_{\lambda_1 + \lambda'_1, \lambda_2 + \lambda'_2} \delta_{\vec{c}}(u - u', v - v'), \phi(u, v)). \end{aligned} \quad (14)$$

If we shift the detector by  $u', v'$  and the source positions by  $-\lambda'_1, -\lambda'_2$ , then there exists another object with the same projection data from the original source and detector positions. Thus, the source positions cannot be identified better than up to a global shift (idem for the detector shifts) from the data only.

**Derivation of the algorithm.** If we write projection data as

$$m_i^l(u, v) = \mathfrak{D}_{\lambda_{1i}, \lambda_{2i}} f^l(u - u_i, v - v_i), \quad (15)$$

$f^l = \sum_{j=1}^4 \delta_{\vec{c}_j^l}$ , then from the moments of order 1 of the type  $M_1^l(i) = (m_i^l(u, v), u)$  and moments of order 2 of the type  $M_2^l(i) = (m_i^l(u, v), u^2)$  we can derive formulas (3), (4), (5). Note that along with the direct calculation of moments for (15), we used that we can compute the same moments with the detected points  $q_{ij}^l$  as  $M_1^l(i) = \frac{D}{(C_3^l)^2} \sum_{j=1}^4 q_{ij}^l$ ,  $M_2^l(i) = \frac{D}{(C_3^l)^2} \sum_{j=1}^4 (q_{ij}^l)^2$ .

## 5 Numerical results

For numerical simulations we launched our algorithm twice: for the first part of the calibration task to find  $\lambda_{1i}, u_i$  and for the second task to find  $\lambda_{2i}, v_i$ . All values of parameters are given in cm:

1. The known parameters of the calibration cage pattern:  $L = 0.4, k_1 = 3, k_2 = 1, k_3 = 2$ . We used the same pattern for the group of vertical sticks and for the group of horizontal sticks.
2. The true positions of sticks:  $p_a = 5, p_b = 8.2, p_c = 4, p_d = 7.2, C_3^a = 8, C_3^b = 9.5, C_3^c = 8, C_3^d = 9.5$ .

3. The true calibration parameters: we randomly selected  $P = 30$  values for source positions in  $[0, 10]$  and fixed  $\lambda_{10} = 0$ . We chose the grid on  $u \in [0, 10]$  with the sampling step 0.01. The detector jitters  $u_i$  were generated as random uniform noise on the interval  $[-0.05, 0.05)$ ,  $u_0 = 0$ . The same was done for the sets of  $\lambda_{2i}, v_i$ .
4. The source-detector distance is fixed  $D = 10$ .

Noise level	Noise std	MAE for $\lambda_{1i}, \lambda_{2i}$	MAE for $u_i, v_i$	MAE for $p_i$	MAE for $C_3^l$
0%	0	$3.86E-13$	$9.67E-14$	$6.50E-14$	$7.65E-14$
10%	0.001	$1.80E-2$	$3.79E-3$	$3.26E-3$	$4.42E-3$
50%	0.005	$1.02E-1$	$2.08E-2$	$1.66E-2$	$2.25E-2$
100%	0.01	$1.89E-1$	$3.76E-2$	$2.82E-2$	$4.37E-2$
200%	0.02	$3.87E-1$	$7.97E-2$	$6.47E-2$	$8.91E-2$

**Table 1:** Mean absolute errors (MAE) for calibration parameters and positions of the markers; all errors are in cm.

In the Table 1 we present the results of our calibration algorithm from two oblique planes. To simulate detection errors, we added to  $q_{ij}^l$  realisations of the Gaussian noise  $N(0, \sigma)$ ,  $\sigma = 0.01 \cdot n_l$ , where  $n_l$  is the noise level, 0.01 is the pixel size of the initial image.

## 6 Conclusion

We have presented a hybrid approach to calibrate cone-beam projections with sources on a plane parallel to the detector with a marker set of partially known geometry and DCCs generalized to compactly supported distributions. We used DCCs on geometric projections of the spherical markers. Thus, DCCs can be computed if projections of the marker set are non-truncated (the rest of the object can be truncated). This is the main advantage of the approach. One disadvantage of our method is the placement of the calibration cage: it has to be parallel to the source and detector planes. Moreover, we see in the Table 1 that our algorithm is sensitive to detection errors. This method requires further numerical simulations and comparisons with other self-calibration methods.

## References

- [1] M. Unberath, A. Aichert, S. Achenbach, et al. "Consistency-based respiratory motion estimation in rotational angiography". *Medical Physics* 44.9 (2017), pp. e113–e124. DOI: [10.1002/mp.12021](https://doi.org/10.1002/mp.12021).
- [2] A. Konik and L. Desbat. "Self-calibration with range conditions for fan-beam on distributions with sources on a line" (2023). *In preparation*.
- [3] A. Konik, L. Desbat, and Y. Grondin. "Hybrid calibration in 3D cone-beam geometry with sources on a line". *Proceedings of the IEEE Nuclear Science Symposium and Medical Imaging Conference*. 2022.
- [4] R. Clackdoyle and L. Desbat. "Full data consistency conditions for cone-beam projections with sources on a plane". *Physics in Medicine and Biology* 58.23 (2013), pp. 8437–8456. DOI: [10.1088/0031-9155/58/23/8437](https://doi.org/10.1088/0031-9155/58/23/8437).